

# DCNN-HBA: Honey Badger Optimization and Deep Convolutional Neural Network Based a Novel Hybrid Model for Producing Quality Image

Sihan Niu<sup>1</sup>, Vineeta Singh<sup>2\*</sup>, Alok Kumar<sup>2</sup>, Deepak Kumar Verma<sup>2</sup>, Sunil Kumar<sup>3</sup>, Vandana Dixit Kaushik<sup>4</sup>, Zhiliang Chen<sup>5</sup> & Kapil Joshi<sup>6</sup>

<sup>1</sup>The Graduate school of Advanced Imaging Science, Multimedia & Film, Chung-Ang University, Seoul, Republic of Korea

<sup>2</sup>Department of Computer Science and Engineering; <sup>3</sup>Department of Information Technology, School of Engineering and Technology (UIET), Chhatrapati Shahu Ji Maharaj University, Kalyanpur, Kanpur 208 024, Uttar Pradesh, India

<sup>4</sup>Department of Computer Science and Engineering, Harcourt Butler Technical University, HBTU East Campus, Nawabganj, Kanpur 208 002, Uttar Pradesh, India

<sup>5</sup>CCTEG Coal Mining Research Institute, Beijing, China

<sup>6</sup>Department of Computer Science and Engineering, Uttarakhand Institute of Technology, Uttarakhand University, Dehradun 248 007, India

*Received 25 August 2023; revised 17 November 2023; accepted 05 December 2023*

The processing of images is a major task in several domains like medical treatment, military, and surveillance. However, the major reasons, like environmental criteria and technical issues made the imperative information tainted. The blurriness represents degradations induced on the image that affected image contrast. There exist several techniques based on image enhancement to improve image quality, but most of these techniques are complex to examine and impose image degradation. An optimized deep technique is devised for producing quality pictures in which the input image is gathered from the database. The pre-processing is done utilizing the median filter to discard the artefacts as well as the noise accumulated in the images. The image enhancement is done with a Deep Convolutional Neural network (DCNN) and the weight update in DCNN is carried out with the Honey Badger Optimization Algorithm (HBA). Thus, the DCNN-HBA helps to enhance the quality of the image without any kind of degradation, like blurriness. The DCNN-HBA technique provides better results with the highest mutual information (MI), highest universal quality index (UQI), maximum UQI, and enhanced efficacy of image enhancement. The highest structural similarity index measurement (SSIM) is the maximum SSIM.

**Keywords:** DCNN, Median filter, Medical imaging, Multi-focus image, Noise removal

## Introduction

The image enhancement is the process of enhancing the acuity or interpretability for the viewers and offers enhanced input. The objective is to alter an image's characteristics to better suit a given task and a specific observer. Here, a number of the image's parameters are improved. The parameters chosen and how they are changed depend on the task at hand. In addition, the observer-specific aspects, like a human visual model and the experience of the observer initiate a huge deal of subjectivity in selecting the image enhancement techniques. It is observed that the enhancement of the image represents the problematic process and its aim is enhancing visual appearance to offer enhanced transform depiction.<sup>1</sup> The enhancement of the image is a technique to maximize the visibility of frequency and minimize the frequency

of image details. It is imperative to enhance the contrast and minimize the noise to maximize the image quality.<sup>1-2</sup> The intention is to enhance the visual image details and offer improved transform modeling for suitable image processing, like recognition, analysis, segmentation, and detection. It also assists in discovering the background data, which is imperative to comprehend the behavior of objects without the involvement of humans. The object fetching from darker background is difficult, due to the low contrast images. The majority of color-based strategies failed if the object color and background were the same.

Several strategies devised to improve the image with the enhancement of gray-level histogram and other techniques are devised based on local contrast transformation with edge assessment and global entropy transformation.<sup>3</sup> This is due to the lack of a general image quality standard, which is considered a design criterion for enhancing the images. There exist

\*Author for Correspondence  
E-mail: vineeta.singh.cs@gmail.com

several methods, which may enhance digital image without destroying it. The enhancement strategies are split into two categories such as Spatial and Frequency Domain, in which the former method directly handles the pixels of images. The values of pixels are modeled to attain the required enhancement. In the latter method, the image is initially transmitted to the frequency domain, which means that the Fourier Transform is evaluated first. These enhancement functions are done to modify the image brightness. Thus, the pixel values of the output image are enhanced by the transformation function adapted to the values of the input. In recent days, huge advancements have been made to boost the quality of images, and the majority of them are devised with DCNN. The current techniques combined DCNN and retinex theory to improve the reflection.

The key intention is to devise an image quality enhancement model utilizing an optimization-enabled deep learning model. The input image is fed to the pre-processing stage employing the median filter to eliminate the noise accumulated in the image. The image enhancement is exhibited utilizing the DCNN. In training DCNN, the weight update is done with HBA to attain the best weights.

Deep learning has facilitated quick design for enhancing image quality, but most of the classical techniques are short of adaptability while focusing on various subtasks. It failed to balance accurate spatial modeling and essential context data. The above issue and challenges of classical techniques are employed as motivation to develop novel models.

The significant contributions of the research involve,

- **Honey Badger Optimization Algorithm:** The HBA optimization is mathematically derived from the behavior of the honey badger and has a high capability in searching strategy that is in both exploration and exploitation balancing. The interaction between the search agents makes it escape from local optima. An efficient optimization should be time-consuming where the digging phase and the honey phase make the proposed model more efficient. These behaviors that are mathematically derived tune the hyper-parameters more efficiently.
- **Deep Convolutional Neural Network-HBA:** The proposed method utilizes HBA for training the DCNN, which may contribute to its ability to capture and enhance important image features effectively. The proposed DCNN model contains

numerous deep layers where the increase in depth makes the network learn more complex and abstract features from the image that assist in providing the image with more enhanced quality.

### Literature Survey

The literature section discusses several existing methodologies for image enhancement, fusion, and denoising, primarily within the domain of medical imaging. The literature survey provides a critical analysis by discussing the method along with its advantages and disadvantages.

Since the image quality relies on the image contrast Stark<sup>4</sup> introduced an image contrast improvement strategy. An adaptive un-sharp masking technique was introduced by Mortezaie *et al.*<sup>5</sup> utilizes image gradients to enhance object details in the image more clearly. The drawback of the method was its prolonged processing time which creates an impact on its practical utility, especially in time-sensitive applications. Hence to reduce the processing time Wang *et al.*<sup>6</sup> incorporated the Residual Hybrid Attention Block (RHAB) into the image enhancement platform. The usage of nested sub-networks for merging multi-scale feature maps added an advantage. However, the absence of loss functions warranted a critical examination of its robustness. A gradient-limited random phase addition technique was used by Zhao *et al.*<sup>7</sup> that blocked the object data diffusion during the image reconstruction process. Even though the model improved the image quality, the method lags in handling different databases. To overcome this Ngo *et al.*<sup>8</sup> addressed this through the usage of light stretch technique. The method's weakness relies on image degradation due to the hue component creates a significant challenge. To improve the image quality Maini and Aggarwal<sup>9</sup> utilized an image enhancement scheme with a roadmap.

A DCNN-based strategy was implemented by Tu *et al.*<sup>10</sup> with the inclusion of reconfigurable computation patterns. In some techniques, focused on multi-focus images or medical images this limitation of scope impacts the effectiveness in handling different types of images or datasets<sup>11-14</sup> Singh and Kaushik<sup>15</sup> developed a novel fusion scheme involving Haar wavelet transform to segregate the images into subparts and a further developed fusion scheme was utilized for producing fusion factors, here medical image dataset has been incorporated for experimenting and simulating results, moreover,

technique has not involve multi-focus images. Thakur *et al.*<sup>16</sup> explored image-denoising tools based on machine-learning approaches that made the image free from noise. The CNN utilized worked well in removing the noise since it is an image.

The human body's internal organs possess complex structures and imaging principles vary from time to time, thus the singular-modality image is not able to provide the full required information, only limited information is gained. In the multi-modality image combination strategy, there is the integration of multi-modal images to produce solitary images which is highly helpful for medical diagnosis purposes. There are many challenges in current fusion techniques such as fusion artifacts, complexity in designing fusion rules, and high computational cost. Here Dogra *et al.*<sup>17</sup> developed a novel fusion strategy to fuse multi-modal medical images for addressing such issues where utilizing a guided filter as well as shearlet transform domain-based statistics of the image. Nanmaran *et al.*<sup>18</sup> developed AI techniques based on a fusion approach much suited for personalized medicine. However, the model took a longer time to execute in comparison with traditional models utilized for cancer classification models. There was further a scope to work on transform-based fusion techniques. Bhutto *et al.*<sup>19</sup> developed a morphological pre-processing technique for addressing irregular illumination as well as noise via the bottom-hat-top-hat technique. The technique provided superior results based on parameters such as image contrast, noise in the final fused image, precise details, and further no information loss. Researchers developed and suggested different techniques in the research field to enhance better quality pictures for medical imaging and research purposes and demonstrated future directions and suggestions to follow.<sup>20-23</sup>

The image quality enhancement is applicable in various domains, Jose *et al.*,<sup>24</sup> used an adolescent identity search algorithm for processing the medical image which is in the NSST domain. For low-light image enhancement, the most efficient LAE-Net was used.<sup>25</sup> In the same way for cassava disease identification, both data augmentation and DL are utilized to enhance the image quality.<sup>26</sup>

### Challenges

Several of the reviewed techniques, including Mortezaie *et al.*<sup>5</sup> and Wang *et al.*<sup>6</sup> faced challenges related to processing time. The efficiency of these methods may be a limitation in real-time applications

or scenarios where quick image processing is essential. Some existing methods face limitations in handling different databases or images this lack of generalizability limits their applicability to different datasets.<sup>7,8</sup> The light stretch technique faced image degradation issues due to the hue component that creates an impact on the method's ability to preserve color information accurately during the enhancement process.<sup>8</sup> In some techniques, focused on multi-focus images or medical images this limitation of scope impacts the effectiveness in handling different types of images or datasets. Some methods faced a lack of utilization of loss functions this absence creates an effect on the robustness and training convergence, which affects the model's performance.

### Proposed Framework

Recently, the majority of people have taken images for recording and sharing their precious instant. However, their images have less dynamic and distorted color tones, because of insufficient lighting circumstances. Thus, the image enhancements turned out to be popular to improve the visual aesthetics of these images. The aim is to devise a technique for enhancing the image quality in which the image is accumulated and fed to pre-processing. Here further median filter has been utilized for discarding the noise. Enhancement of image is done with DCNN in which DCNN training is performed using HBA. The structural design of the image enhancement with DCNN-HBA technique has been portrayed through Fig. 1.

Let us suppose we have a dataset  $F$  possessing  $d$  source images that may be expressed via following

$$F = \{H_l ; 1 \leq l \leq d\} \quad \dots (1)$$

where,  $H_l$  depicts  $l^{\text{th}}$  image. Further, the image  $H_l$  has been imposed for the pre-processing phase.

### Pre-Processing with Median Filter

Here the source image  $H_l$  is inputted for pre-processing where a median filter has been imposed for discarding noise. The median filter is reliable and easy to implement as it has a simple structure. In addition, the filter is a non-linear representation utilized to eliminate the noisy signal and is formulated as,

$$A = \text{median}_{(H_l) \in D} \{g(H_l)\} \quad \dots (2)$$

The median filter output after pre-processing is denoted as  $A$ , and it is further utilized for image

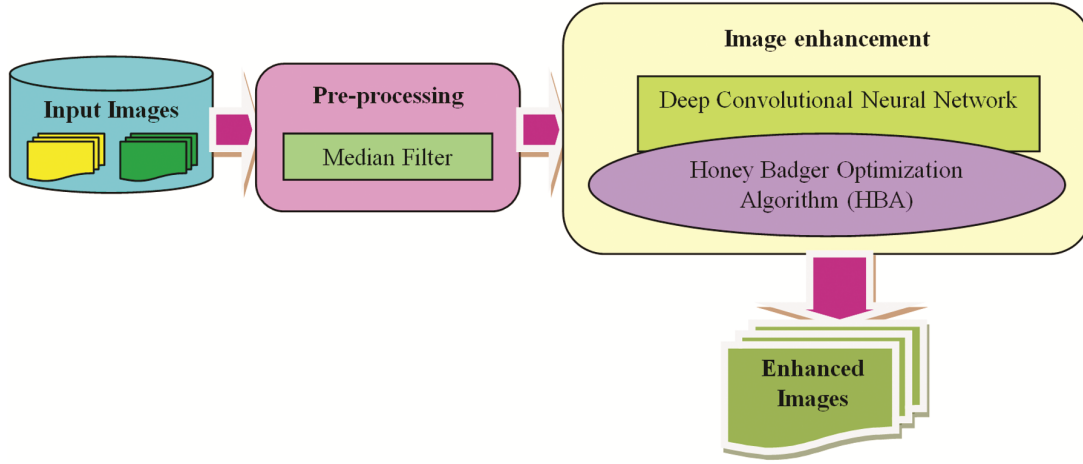


Fig. 1 — Structure of image enhancement model using HBA-based Deep CNN

enhancement, the input image is expressed as  $H_i$  and  $D$  refers database.

#### Image Enhancement using HBA-Based DCNN

The pre-processed output  $A$  is adapted as DCNN<sup>10</sup> input. Here, the training of DCNN is done with HBA. The image enhancement is done to elevate the image contrast. Here, the enhancement of the image is done with DCNN in which DCNN training is performed with HBA. The DCNN structure and training of DCNN with HBA are illustrated below.

#### Structure of DCNN

DCNN consists of a connected layer, a convolutional layer, abbreviated as conv, Pooling in short named POOL as well as a fully connected (FC) layer. The DCNN is utilized for identifying the relevant information from the images. The DCNN can handle a huge number of features. In addition, it is effective in dealing with the unstructured data. The conv layer intends to generate feature maps with pre-processed images  $A$  and the generated pre-processed images are sub-sampled with the pooling layer. The DCNN structure is revealed in Fig. 2. The term "Deep Convolutional Neural Network" denotes the depth or the number of layers in a CNN. A DCNN has a larger number of layers compared to a traditional CNN. The increase in depth makes the network learn more complex and abstract features. In the proposed model the DCNN contains a total of three convolutional layers, batch normalization layers and ReLU layers, two max pooling layers in 2D, one fully connected layer, and a softmax layer.

i) **Convolutional Layer:** The layer employs the pre-processed images  $A$  and this layer represents

neuron connections and it generates a feature map. The convolution layers are given by,

$$D = \{D_1, D_2, \dots, D_u, \dots, D_e\} \quad \dots (3)$$

where,  $e$  expressing the number of the convolutional layer,  $D_u$  depicts  $u^{\text{th}}$  convolutional layer. Further the convolutional outcome at  $(q, v)$  units may be expressed via,

$$(G_h^r)_{q,v} = (K_h^r)_{q,v} + \sum_{\alpha=1}^{E_1^{w-1}} \sum_{\beta=-a_1^c}^{a_1^c} \sum_{\gamma=-a_2^c}^{a_2^c} (B_{b,l}^r)_{1,0} * (C_l^{r-1})_{q+1,v+0} \quad \dots (4)$$

Here,  $E_1^{w-1}$  depicts the total feature map out of the prior convolutional layer,  $*$  indicates the convolutional operator as well as  $(G_l^{r-1})_{q+1,v+0}$  represents the fixed feature map. In addition,  $(B_{b,l}^r)_{1,0}$  is the weight of the network, which is trained by HBA and builds the weight of  $r^{\text{th}}$  convolutional layer.

ii) **Pooling Layer:** The layer ensures the efficiency of adapting the activation function and straight forwardness in vast network processes. Its result is subjected to a feature map, and is given by,

$$G_h^r = \text{fun}(G_h^{r-1}) \quad \dots (5)$$

where,  $\text{fun}()$  is the activation function. Furthermore, the pooling layer efficiently minimizes system complexity.

iii) **Fully Connected Layers:** The classification result generated with the convolutional layer and pooling layer is fed to the input of the FC layer, for high-level reasoning. Finally, the FC output is given as,

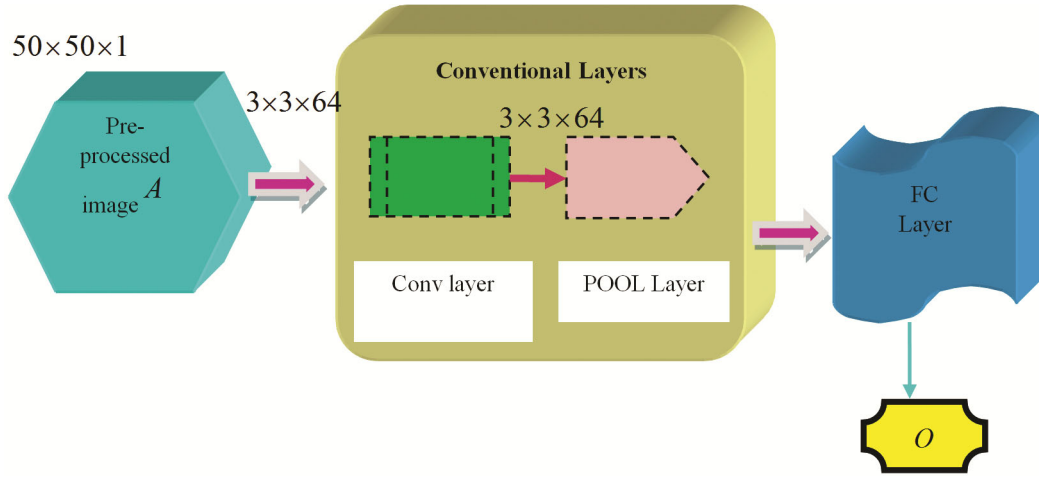


Fig. 2 — Structural diagram of DCNN

$$I_h^r = (L_h^r) \text{ with } L_h^r = \sum_{\alpha=1}^{E_1^{r-1}} \sum_{\beta=a_1^r}^{E_2^{r-1}} \sum_{\gamma=a_2^r}^{E_3^{r-1}} (Q_{h,\alpha,q,v}^r) \cdot (G_h^{r-1})_{q,v} \quad \dots (6)$$

Here,  $Q_{h,\alpha,q,v}^r$  is weight related to  $(q,v)$  in  $I^h$  feature map of layer  $r-1$ , and  $h^{th}$  element in  $r^{th}$  layer. Here, the output from DCNN is expressed as  $O$ .

**Training of DCNN with HBA**

Here deep convolution neural network training has been done with honey badger optimization.<sup>27</sup> The HBA was developed with honey badgers' shrewd foraging characteristics in mind. The honey badger's active hunting style as well as honey and digging discovery techniques are modified. With the search policy, the HBA successfully addresses the optimization issues. The technique used to create the HBA paradigm is depicted as,

i) *Initiation*: In starting, the population size  $E$  and associated positions are used to initialize the number of honey badgers as follows:

$$S_c = T_c + \omega_1 \times (M_c - T_c) \quad \dots (7)$$

where,  $S_c$  depicts  $c^{th}$  honey badger location in total population,  $T_c$  stands for lower bounds,  $M_c$  stands for upper bound, whereas  $\omega_1$  depicts random number among 0 and 1.

ii) *Procedure of Fitness Function Computation*: The fitness with the lowest value is considered the best option for picture enhancement in this case when fitness is calculated to find the required ideal solution. Creation of a fitness function that takes error into account,

$$\xi = \frac{1}{r} \sum_{\sigma=1}^r (N_r^* - O)^2 \quad \dots (8)$$

In equation (8),  $r$  denotes the number of samples in the dataset, whereas  $N_r^*$  denotes the target output, moreover  $O$  is the DCNN output, as well as the fitness function depicted via  $\xi$ .

iii) *Describing Intensity*: Intensity reveals two things: prey size as well as the distance between the  $r^{th}$  prey and  $r^{th}$  honey badger. The inverse square law, which describes movement, states that it happens quickly if the smell is strong. According to its definition,

$$P_c = \omega_2 \times \frac{U}{4 \pi v_c^2} \quad \dots (9)$$

where,  $\omega_2$  depicts random value between 0 and 1,  $U$  denotes concentration strength, whereas  $v_c$  reveals distance amongst  $c^{th}$  honey badger as well as prey. However, the following expression depicts the term  $U$  and  $v_c$ .

$$U = (S_c - S_{c+1})^2 \quad \dots (10)$$

where,  $S_c$  denotes  $c^{th}$  honey badger location and  $S_{c+1}$  denotes  $c+1^{th}$  honey badger location.

$$v_c = S_{prey} - S_c \quad \dots (11)$$

where,  $S_{prey}$  signifies the position of prey.

iv) *Updating Density Factor*: This density factor facilitates handling time-fluctuating randomization to ensure smoother evolution from exploitation to exploration. For the below equation to reduce

randomness over time, the density factor lowers as iterations progress.

$$\rho = Z \times \exp \left( \frac{-a}{a_{\max}} \right) \quad \dots (12)$$

where,  $Z$  depicts constant, while  $a_{\max}$  stands for the highest number of iterations.

v) *Escape the Local Optimum*: This technique utilizes a flag  $R$ , that alters the direction of search to reward elevated prospects for agents to scan search space rigorously.

vi) *Location of Agents being Updated*: The two primary phases of the HBA position updating process are the "digging" phase and the "honey phase," explained below:

a) **Digging Stage**:- The honey badger's motion resembles a cardioid, and the movement of the cardioids is caused by,

$$S_{\text{new}} = S_{\text{prey}} + R \times \varepsilon \times E \times S_{\text{prey}} + R \times \omega_3 \times \rho \times v_c \times |\cos(2\pi\omega_4) \times [1 - \cos(2\pi\omega_5)]| \quad \dots (13)$$

where,  $S_{\text{prey}}$  refers to the prey's location,  $\varepsilon \geq 1$ ,  $\omega_3$ ,  $\omega_4$  and  $\omega_5$  are random numbers among 0 and 1. Moreover  $R$  operates as a flag, which varies search direction and is identified by,

$$R = \begin{cases} 1 & , \text{if } \omega_6 \leq 0.5 \\ -1 & , \text{else} \end{cases} \quad \dots (14)$$

where,  $\omega_6$  stands for random integer in the range between 0 and 1. Furthermore, a honey badger depends upon low-intensity  $E$  for  $S_{\text{prey}}$ . Whereas, badgers can gain any difficulty  $R$  in the activity of digging, which further allows for identifying optimal prey locations.

b) **The Honey Phase**: Here the source is stimulated by equation (15) when the honey badger undergoes honeyguide bird to reach the beehive,

$$S_{\text{new}} = S_{\text{prey}} + R \times \omega_7 \times \rho \times v_c \quad \dots (15)$$

where,  $S_{\text{new}}$  shows the updated location of honey badger, while  $\omega_7$  illustrating a random integer in between 0 and 1.

vii) *Evaluating Solution Feasibility*: Here the optimal solution is attained through the fitness, which is

described in equation (8), where the fitness function has the least possible value and is taken as the optimum solution.

viii) *Termination*: Here aforementioned algorithmic phases are executed constantly until the highest solution is gained.

The output generated with DCNN-HBA is expressed as  $O$ , which is the enhanced image.

## Experimental Setup and Results

Here the efficacy of the DCNN-HBA model is demonstrated in terms of MI, UQI, and SSIM. The DCNN-HBA model has been implemented in MATLAB with OS Windows 10, Intel I3 core processor along with 2GB RAM. The performance evaluation of techniques is performed on BRATS 2018 dataset images and lytro multi-focus images. The BRATS 2018 dataset<sup>28</sup> comprises MRIs along with brain tumor segmentation involving ground truth samples possessing four MRI modalities as T1, T1c, T2, and FLAIR. Additionally, the medical images have been accumulated from 19 institutions involving distinct MRIs. The Lytro Multi-focus image Dataset<sup>29</sup> includes 20 multi-focus colored pictures in pairs, with an individual  $520 \times 520$  pixels image size and four arrangements of multi-focus colored pictures utilizing three sources. The efficiency of HBA-based DCNN is examined via different assessment parameters utilizing the MI, SSIM, and UQI. The parameter settings that create a significant impact are as follows, The population size is 50 with a maximum iteration of 1000, the ReLU activation function is utilized, and the catch size of 64.

a) **MI**: Here mutual information represents two arbitrary variables is mutual dependence amongst two variables and it quantifies the amount of information, which is formulated as,

$$I(B : Y) = H(B) - H(B | Y) \quad \dots (16)$$

where,  $H(B)$  refers to entropy of  $B$ , conditional entropy of  $B$  given  $Y$ .

b) **UQI**: The UQI is utilized to model any type of distortion in an image considering luminance, contrast, and structural comparisons, which is expressed as,

$$UQI(z, b) = p(z, b), q(z, b), r(z, b) \quad \dots (17)$$

where,  $r(z, b)$ ,  $p(z, b)$ , and  $q(z, b)$  represents structure, luminance as well as contrast of images.

c) **SSIM:** It serves as a means of validating the visual model that has been imposed for contrast, structure as well and luminance data. Mathematically SSIM is provided via the following expression:

$$B = [ p(z, b) ]^\alpha [ q(z, b) ]^\beta [ r(z, b) ]^\eta \dots \quad (18)$$

where,  $p(z,b)$ ,  $q(z,b)$  and  $r(z,b)$  signifies luminance, contrast, and image structures, and the attribute  $\alpha$ ,  $\beta$ , and  $\eta$  are fixed to 1.

**Experimental Outcomes**

Experimental outcomes of DCNN-HBA with images acquired from database-1 and database-2 have

been displayed in Fig. 3 and Fig. 4 respectively. The set of input images considered is displayed in Fig. 3a). Fig. 3b) presents the noise-added image. Fig. 3c) presents the filtered image. The output image is denoted in Fig. 3d). The experimental results of the DCNN-HBA model with a group of images from database-2 are displayed in Fig. 4. The set of input images employed is depicted in Fig. 4a. Fig. 4b presents the noise-added image. Fig. 4c presents the filtered image. The output image is presented in Fig. 4d).

**Comparative analysis**

Here the DCNN-HBA model has been evaluated with recent state-of-art techniques involving AISA<sup>24</sup>,

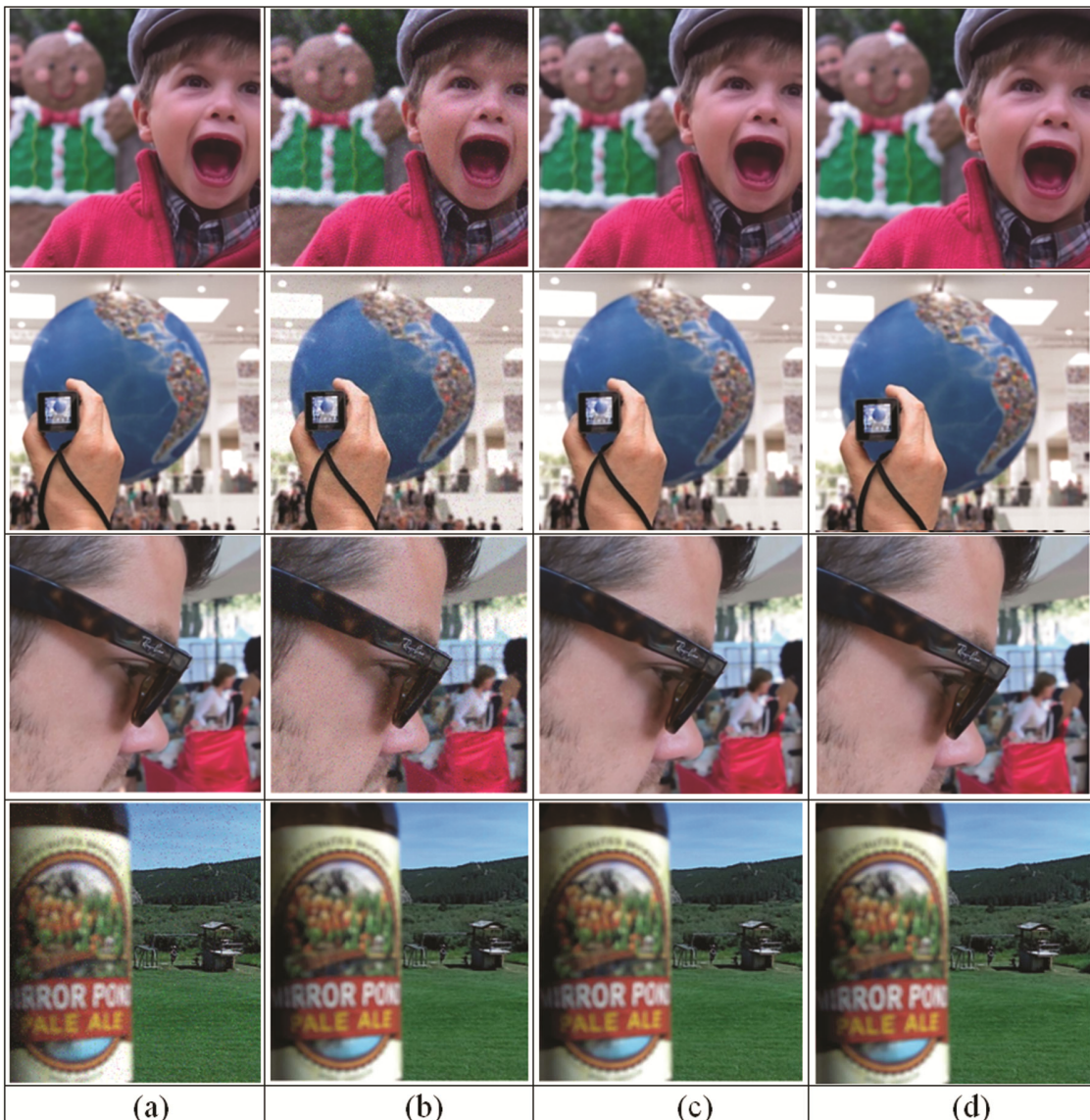


Fig. 3 — Experimental outcomes of HBA-based DCNN with Dataset-1 considering (a) Source image, (b) Noise added image, (c) Filtered image, and (d) Output image

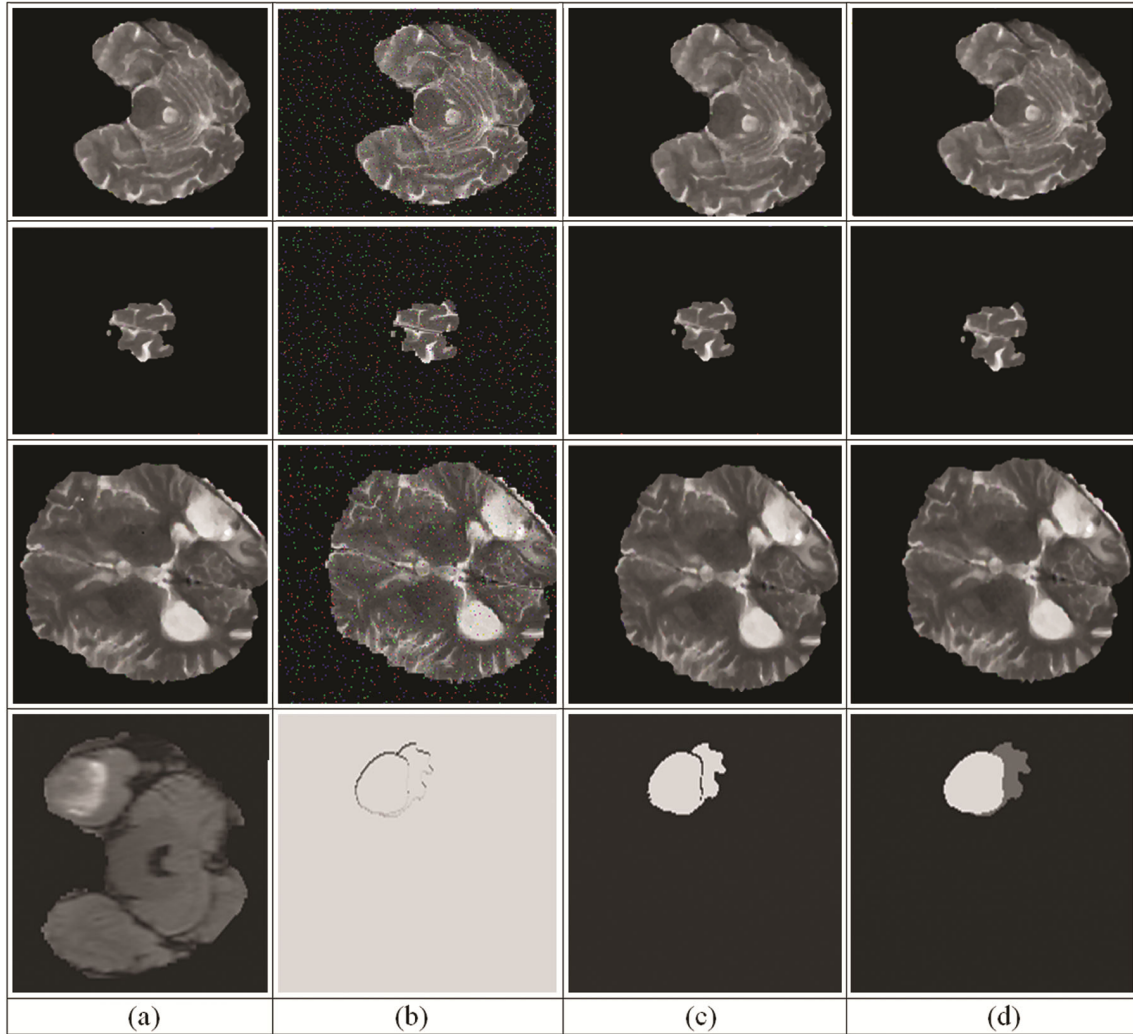


Fig. 4 — With Dataset-2 considering (a) Source image, (b) Noise added image, (c) Filtered image, and (d) Output image

LAE-NET<sup>25</sup>, DRL<sup>30</sup>, GAN<sup>31</sup>, CNN<sup>32</sup>. The efficacy of the DCNN-HBA has been shown in terms of MI, SSIM along UQI with BRATS and Lytro Multi-focus Image. The analysis is done by generating the wavelets which include Daubechies 2 (db1), and Daubechies 2 (db2) wavelets of image wherein the image is obtained from the dataset.

#### *Assessment with Db1 Wavelet (Using Dataset1)*

The assessment of techniques with db1 wavelet for dataset1 involving different numbers of images has been displayed via Fig. 5. The assessment considering MI is depicted in Fig. 5a. The assessment considering UQI and SSIM is illustrated in Fig. 5b and Fig. 5c respectively.

#### *Assessment with Db2 Wavelet (Using Dataset2)*

The assessment of techniques for dataset2 with db2 wavelet considering different counts of

images is depicted in Fig. 6. The assessment that takes MI into account is exposed in Fig. 6a. The assessment that takes UQI into account is revealed in Fig. 6b. The assessment that takes SSIM into account is revealed in Fig. 6c.

#### *Comparative Discussion*

The comparative discussion for Dataset-1 is tabulated in Table 1 and the comparative results for Dataset-2 are tabulated in Table 2. The HBA that is mathematically derived optimally performs the hyperparameter tuning. By utilizing the foraging strategies of HBA, the algorithm can effectively adjust CNN hyperparameters, leading to improved model performance. The developed DCNN-HBA consistently outperformed DRL, GAN, and CNN in terms of MI across various images in both

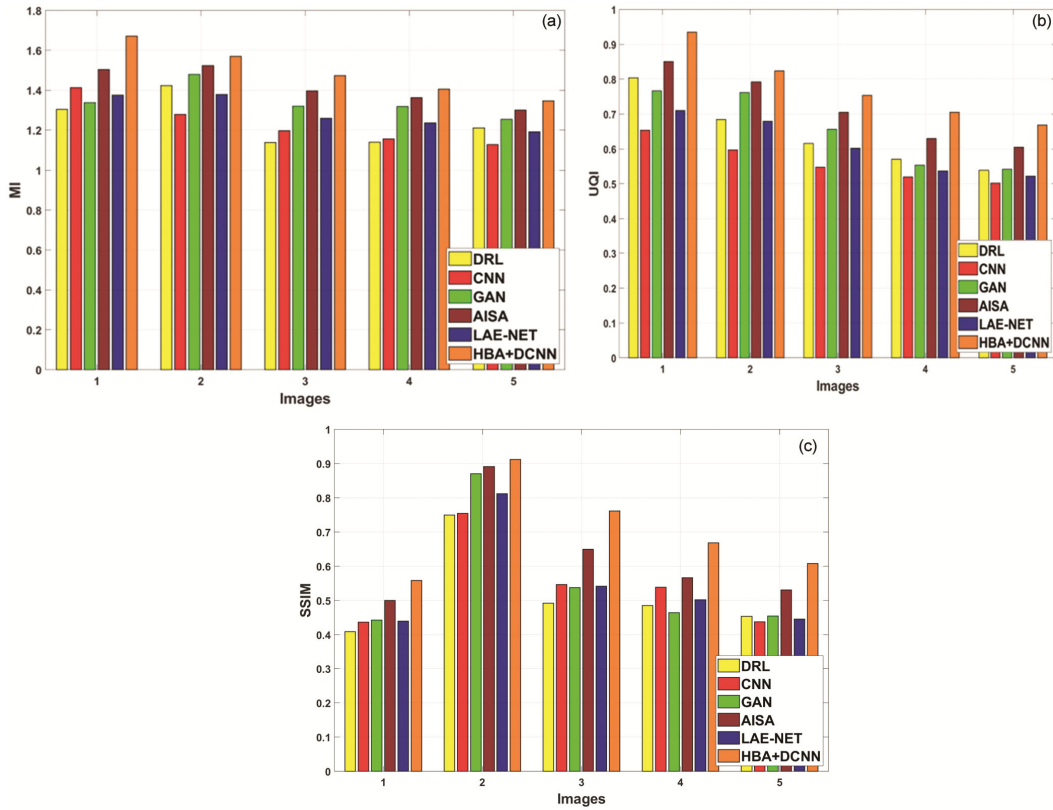


Fig. 5 — Analysis of Techniques with Dataset1 using Db1 Wavelet Considering (a) MI, (b) UQI, and (c) SSIM

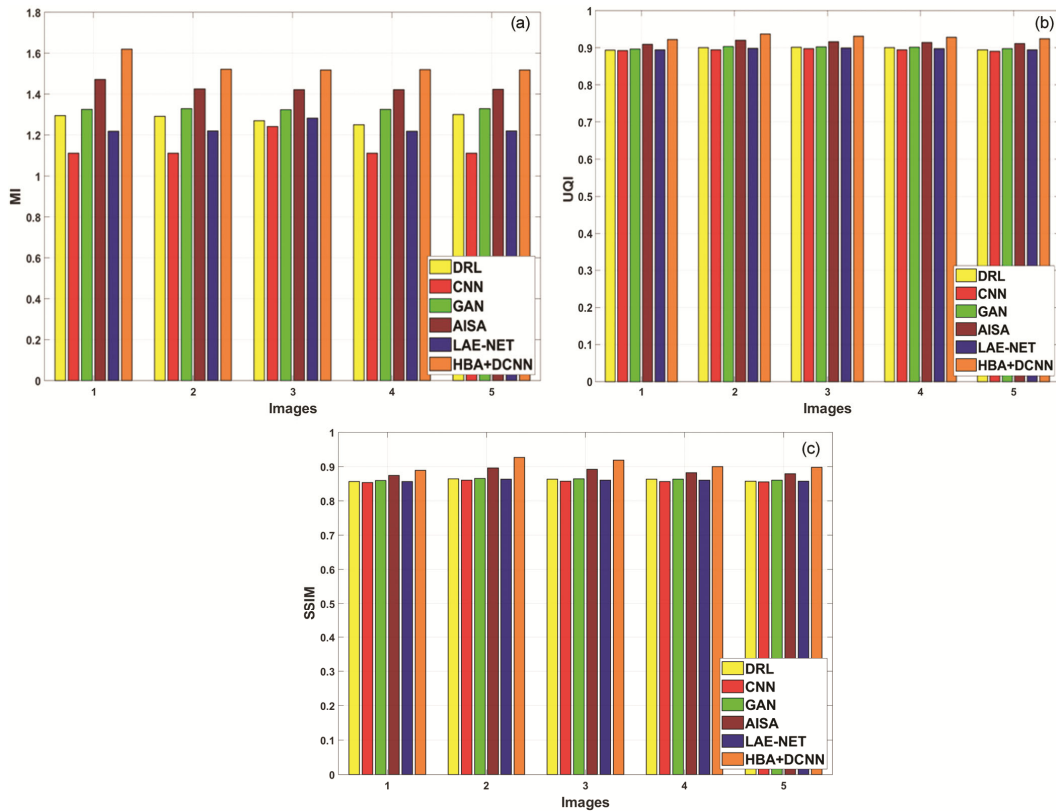


Fig. 6 — Assessment of Techniques with Dataset2 with Db2 Wavelet using (a) MI, (b) UQI, and (c) SSIM

Table 1 — Comparative Assessment Using Db1 wavelet for Dataset-1

Image	Metrics	AISA <sup>24</sup>	LAE-NET <sup>25</sup>	DRL <sup>30</sup>	GAN <sup>31</sup>	CNN <sup>32</sup>	Proposed HBA+DCNN
1	MI	1.505	1.375	1.304	1.338	1.413	1.672
2	MI	1.524	1.379	1.424	1.479	1.280	1.569
3	MI	1.397	1.259	1.138	1.321	1.197	1.474
4	MI	1.362	1.237	1.141	1.318	1.156	1.406
5	MI	1.301	1.191	1.212	1.255	1.128	1.347
1	UQI	0.851	0.710	0.804	0.767	0.653	0.935
2	UQI	0.792	0.679	0.684	0.761	0.597	0.823
3	UQI	0.705	0.601	0.615	0.656	0.547	0.754
4	UQI	0.629	0.536	0.570	0.553	0.519	0.705
5	UQI	0.604	0.521	0.538	0.541	0.502	0.668
1	SSIM	0.500	0.439	0.408	0.442	0.436	0.558
2	SSIM	0.891	0.812	0.749	0.870	0.754	0.912
3	SSIM	0.649	0.542	0.492	0.537	0.546	0.761
4	SSIM	0.566	0.501	0.485	0.464	0.539	0.668
5	SSIM	0.531	0.446	0.453	0.454	0.437	0.607

Table 2 — Comparative Assessment for Comparative Assessment Using Db2 for Dataset2

Image	Metrics	AISA <sup>24</sup>	LAE-NET <sup>25</sup>	DRL <sup>30</sup>	GAN <sup>31</sup>	CNN <sup>32</sup>	Proposed HBA+DCNN
1	MI	1.473	1.219	1.296	1.325	1.112	1.620
2	MI	1.426	1.221	1.292	1.329	1.112	1.522
3	MI	1.422	1.283	1.270	1.324	1.241	1.519
4	MI	1.422	1.219	1.251	1.325	1.112	1.519
5	MI	1.424	1.221	1.301	1.329	1.112	1.518
1	UQI	0.909	0.894	0.893	0.896	0.892	0.922
2	UQI	0.920	0.898	0.900	0.902	0.894	0.937
3	UQI	0.916	0.899	0.901	0.902	0.897	0.931
4	UQI	0.914	0.897	0.900	0.901	0.894	0.927
5	UQI	0.911	0.894	0.894	0.897	0.890	0.924
1	SSIM	0.874	0.856	0.856	0.859	0.853	0.889
2	SSIM	0.896	0.863	0.864	0.865	0.860	0.927
3	SSIM	0.892	0.861	0.863	0.865	0.857	0.919
4	SSIM	0.882	0.860	0.863	0.864	0.857	0.900
5	SSIM	0.879	0.858	0.857	0.860	0.855	0.898

datasets, especially with the highest MI values of 1.672 for db1 and 1.620 for db2. This indicates a significant reduction in uncertainty and improved information capture by the proposed model. The median filter used in the research removes the noise present in the images which creates a huge impact in UQI. The UQI results reveal the efficacy of HBA-DCNN model in managing image quality. The highest UQI values are achieved by DCNN-HBA for both db1 and db2 wavelets across different image pairs and datasets. This suggests that the proposed method performs well in preserving image quality during enhancement. The SSIM results further certify the domination of the DCNN-HBA method. Across various images and datasets, the DCNN-HBA model consistently achieved the highest SSIM values 0.912 for db1 and 0.927 for db2. High SSIM values indicate improved outcomes with decompressed images, emphasizing the efficacy of the model in enhancing structural similarity.

Table 3 — Time Complexity Analysis

Methods	Time (ms)
AISA <sup>24</sup>	25
LAE-NET <sup>25</sup>	29
DRL <sup>30</sup>	26
GAN <sup>31</sup>	27
CNN <sup>32</sup>	22
Proposed HBA+CNN	20

Table 4 — Analysis Based on Loss

Methods	Dataset-1	Dataset-2
AISA <sup>24</sup>	0.051	0.029
LAE-NET <sup>25</sup>	0.044	0.021
DRL <sup>30</sup>	0.079	0.030
GAN <sup>31</sup>	0.060	0.037
CNN <sup>32</sup>	0.062	0.024
Proposed HBA+CNN	0.037	0.008

**Analysis based on Time**

To reveal the effectiveness of the DCNN-HBA model the computation time is analyzed along with the existing method and is visually displayed in Table 3 and the convergence graph is displayed in Fig. 7 and tabulated in Table 4.

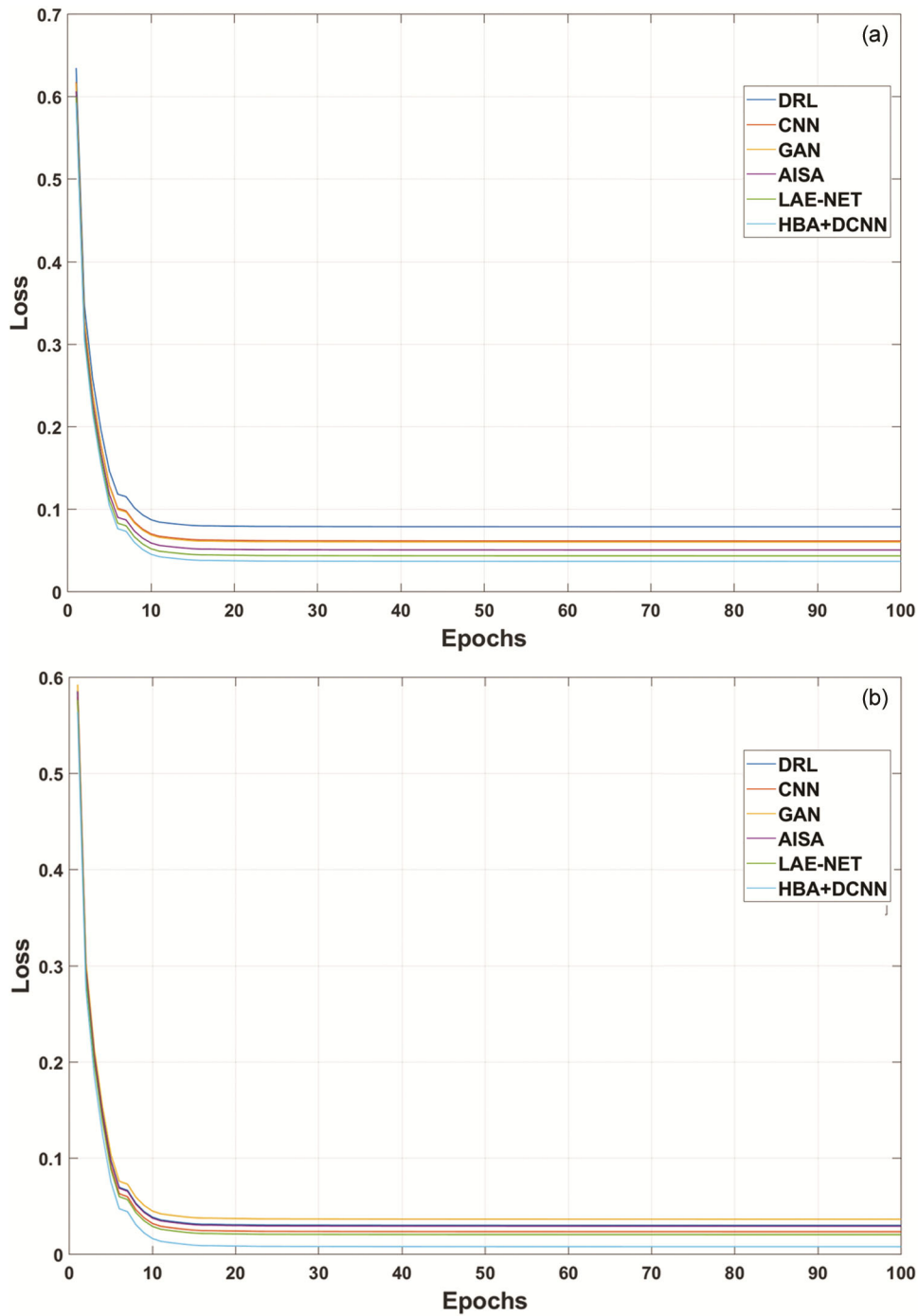


Fig. 7 — Convergence graph (a) Dataset-1, and (b) Dataset-2

**Conclusions**

The research proposed an optimization technique along with DCNN, utilizing an DCNN-HBA for enhancing image quality. Here two datasets are utilized it undergoes pre-processing to eliminate noise, accomplished through the application of a median filter to discard artifacts. The utilization of the

DCNN-HBA in the image enhancement process ensures that the method not only avoids degradation such as blurriness but also enhances the network's capability to handle intricate degradation kernels by adapting to ensure efficiency. Notably, the proposed technique demonstrates superior results, evidenced by the highest Mutual Information MI, UQI and highest

SSIM. Significantly, the proposed model achieves these outcomes while remaining free from degradation and effectively minimizing blurriness, ultimately producing images of exceptional quality. Furthermore, the suggested model will be enhanced to handle several image types, including multi-exposure images, thereby expanding its versatility and applicability in the future.

## References

- 1 Agaian S S, Panetta K & Grigoryan A M, A new measure of image enhancement, In *IASTED Int Conf Signal Proc Communication, Citeseer*, (2000) 19–22.
- 2 Ballard D and Brown C, *Computer Vision, Englewood Clifid, Prentice-Hall*, (1982).
- 3 Agaian S S, Visual Morphology, *Proceedings of SPIE, Nonlinear Image Processing X, San Jose CA*, **3304** (1999) 153–163.
- 4 Stark J A, Adaptive image contrast enhancement using generalizations of histogram equalization, *IEEE Trans Image Process*, **9(5)** (2000) 889–896.
- 5 Mortezaei Z, Hassanpour H & Asadi Amiri S, An adaptive block based Un-sharp masking for image quality Enhancement, *Multimed Tools Appl*, **78(16)** (2019) 23521–23534.
- 6 Wang J, Yang Y & Hua Y, Image quality enhancement using hybrid attention networks, *IET Image Process*, **16(2)** (2022) 521–534.
- 7 Zhao T, Liu J, Duan J, Li X & Wang Y, Image quality enhancement via Gradient-limited random phase addition in holographic display, *Opt Commun*, **442** (2019) 84–89.
- 8 Ngo D, Lee S and Kang B, Light stretch algorithm for image quality enhancement, In *Proceedings of the 4th International Conference on Virtual Reality*, (2018) 56–60.
- 9 Maini R and Aggarwal H A, Comprehensive review of image enhancement techniques, (2010), *arXiv preprint arXiv:1003.4053*.
- 10 Tu F, Yin S, Ouyang P, Tang S, Liu L & Wei S, Deep convolutional neural network architecture with reconfigurable computation patterns, *IEEE Trans Very Large Scale Integr (VLSI) Syst*, **25(8)** (2017) 2220–2233.
- 11 Singh V & Kaushik V D, Renyi entropy and atom search sine cosine algorithm for multi focus image fusion, *Signal Image Video Process*, **15** (2021) 903–12.
- 12 Singh V & Kaushik V D, HoEnTOA: Holoentropy and Taylor assisted optimization based a novel image quality enhancement algorithm for multi-focus image fusion, *J Sci Ind Res*, **80(10)** (2021) 875–886.
- 13 Singh V and Kaushik VD, WeAbDeepCNN: Weighted average model and ASSCA based two level fusion scheme for multi-focus images, *J Sci Ind Res*, **80(10)** (2021) 905–914.
- 14 Singh V and Kaushik V D, DTCWTASODCNN: Dual tree complex wavelet transform based weighted fusion model for multi-modal medical images quality improvement with atom search optimization technique & deep cnn, *J Sci Ind Res*, **81(08)** (2022) 850–858.
- 15 Singh V and Kaushik V D, Haar Adaptive Taylor-ASSCA-DCNN: Some novel fusion model for image quality enhancement, *J Sci Ind Res*, **82(5)** 2023 568-578.
- 16 Thakur R S, Chatterjee S, Yadav R N and Gupta L, Image de-noising with machine learning: A Review, *IEEE Access*, **9** (2021) 93338–93363.
- 17 Dogra A & Kumar S, Multi-modality medical image fusion based on guided filter and image statistics in multidirectional shearlet transform domain, *J Ambient Intell Humaniz Comput*, **14** (2022) 1–15.
- 18 Nanmaran R, Srimathi S, Yamuna G, Thanigaivel S, Vickram A S, Priya A K, Karthick A, Karpagam J, Mohanavel V & Muhibbullah M, Investigating the role of image fusion in brain tumor classification models based on machine learning algorithm for personalized medicine, *Comput Math Methods Med*, **2022** (2022) 7137524.
- 19 Bhutto J A, Tian L, Du Q, Sun Z, Yu L & Tahir M F, CT and MRI medical image fusion using noise-removal and contrast enhancement scheme with convolutional neural network, *Entropy*, **24(3)** (2022) 393.
- 20 Amanlou A, Suratgar A A, Tavvoosi J, Mohammadzadeh A & Mosavi A, Single-image reflection removal using deep learning: A systematic review, *IEEE Access*, (2022).
- 21 Saniour I, Robb F J, Taracila V, Mishra V, Vincent J, Voss H U & Winkler S A, Characterization of a low-profile, flexible, and acoustically transparent receive-only mri coil array for high sensitivity mr-guided focused ultrasound, *IEEE Access*, (2022).
- 22 Bai Y, Zhu Z, Zhu C, & Wang Y, Blind image quality assessment of screen content images via fisher vector coding, *IEEE Access*, **10** (2022) 13174–13181.
- 23 Imamura T, Baba M, Hoshikawa N, Nakayama H, Ito T & Shiraki A, A new algorithm for displaying images with high resolution using a directional volumetric display with threads and a projector, *IEEE Access*, **10** (2022) 15288–15297.
- 24 Jose J, Gautam N, Tiwari M, Tiwari T, Suresh A, Sundararaj V & Rejeesh M R, An image quality enhancement scheme employing adolescent identity search algorithm in the NSST Domain for multimodal medical image fusion, *Biomed Signal Process Control*, **66** (2021) 102480.
- 25 Liu X, Ma W, Ma X & Wang J, LAE-Net, A locally-adaptive embedding network for low-light image enhancement, *Pattern Recognit*, **133** (2023) 109039.
- 26 Abayomi-Alli O O, Damaševičius R, Misra S & Maskeliūnas R, Cassava disease recognition from low-quality images using enhanced data augmentation model and deep learning, *Expert Syst*, **38(7)** (2021) e12746.
- 27 Hashim F A, Houssein E H, Hussain K, Mabrouk M S and Al-Atabany W, Honey Badger Algorithm: New metaheuristic algorithm for solving optimization problems, *Math Comput Simul*, **192** (2022) 84–110.
- 28 BRATS dataset has been taken from, “<https://www.med.upenn.edu/sbia/brats2018/data.html>”, accessed on November 2022.
- 29 Lytro Multi-focus Image Dataset has been taken from, “[https://www.researchgate.net/publication/291522937\\_Lytr0\\_Multi-focus\\_Image\\_Dataset](https://www.researchgate.net/publication/291522937_Lytr0_Multi-focus_Image_Dataset)”, accessed on November 2022.
- 30 Zhang R, Guo L, Huang S and Wen B, ReLLIE: Deep Reinforcement Learning for customized low-light image enhancement, In *Proceedings of the 29th ACM International Conference on Multimedia*, (2021) 2429–2437.
- 31 Guo Y, Li H and Zhuang P, Underwater image enhancement using a multiscale dense generative adversarial network, *IEEE J OceanEng*, **45(3)** (2019) 862–870.
- 32 Tao L, Zhu C, Song J, Lu T, Jia H & Xie X, Low-light image enhancement using cnn and bright channel prior, In *Proceedings of IEEE International Conference on Image Processing (ICIP)*, (2017) 3215–3219.